

BELLCOMM, C.
955 L'ENFANT PLAZA NORTH, S.W. WASHINGTON, D. C. 20524

SUBJECT: Attitude Control for AAP 1/2 and
AAP 2/3A: A Progress Report
Case 620

DATE: March 10, 1969
FROM: J. J. Fearnside

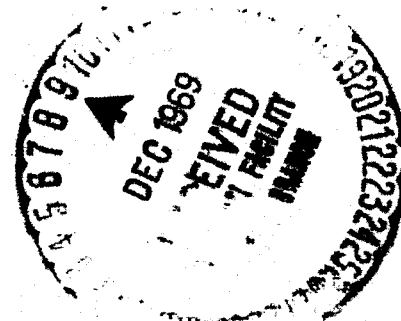
ABSTRACT

Preliminary results are presented for a thruster firing control law for holding X-POF attitude in missions AAP 1/2 and AAP 2/3A. It is shown that significant reductions in the number of thruster ignitions and in the amount of propellant consumption can be achieved if a control strategy is used in which the gravity-gradient and aerodynamic torques produce a bounded oscillatory attitude motion about all three spacecraft axes.

N70-11735

FACILITY FORM 602

(ACCESSION NUMBER)	_____	(THRU)	_____
(PAGES)	20	(CODE)	1
(NASA OR OR TMX OR AD NUMBER)	CL# 106962	(CATEGORY)	21



BELLCOMM, INC.

955 L'ENFANT PLAZA, NORTH, S.W.

WASHINGTON, D. C. 20024

SUBJECT: Attitude Control for AAP 1/2 and
AAP 2/3A: A Progress Report
Case 620

DATE: March 10, 1969

FROM: J. J. Fearnside

MEMORANDUM FOR FILE

I. INTRODUCTION

A recent study^{(1)*} for MSFC by IBM indicates that, in order to maintain the Orbital Assembly (OA) in the POP mode during missions AAP 1/2 and AAP 2/3A, the Workshop Attitude Control System (WACS) must provide a total impulse per orbit of 100 pound-seconds and fire the thrusters an average of 80 times per orbit. These figures, when calculated over 16 orbits per day and a combined mission duration of 84 days, represent 500 pounds of propellant and 107,520 thruster firings. The baseline figure of 220,000 pound-seconds of total impulse represents 815 pounds of fuel. The maintenance of the POP mode, therefore, is estimated to expend over 60% of the total impulse. Further, the thruster-ignition estimate is such as to cause concern about the reliability of the reaction control system.

The following presents a physically-motivated control strategy which could significantly reduce the aforementioned measures of control system performance. The basic strategy is to cause the thrusters to synchronize the motion in such a way as to have the turning points of the attitude motion produced by the gravity-gradient and aerodynamic torques acting on the spacecraft. This strategy is applied to all three axes and leads to a "natural" selection of deadbands. For the OA these deadbands are approximately $\pm 9.5^\circ$ for the long axis of the vehicle, which is nominally perpendicular to the orbit plane (POP), and $\pm 4^\circ$ for the axes that are nominally in the orbit plane. The maximum rates are on the order of 19.5×10^{-3} degrees per second for the long axis and 5×10^{-3} degrees per second for the others. These figures depend, of course, on the moments of inertia of the spacecraft and on the magnitude of the disturbances.

The result of applying this control strategy to the OA in the POP mode is a reduction in control system activity which is so significant that, under ideal conditions and

* Superscripted numbers indicate references listed at the end of the report.

assuming no diurnal bulge in the model of the atmospheric density,* only the initialization process requires any propellant consumption or thruster firings.

A more detailed exposition of this idea is given in subsequent sections: Section II discusses some of the physical principles which motivated this strategy; Section III consists of a pertinent illustrative example which is free of mathematical difficulty; Section IV is concerned with the application to an idealized representation of the OA; and Section V considers some practical matters and initial thoughts on the implementation of this strategy. Appendix A demonstrates the method of successive approximations which is used to apply this control policy to the rather complicated equations of motion of a spacecraft in the POP mode.

II. A PHYSICAL APPROACH TO OPTIMIZATION

The first step in the design of a fuel-optimal control strategy for steady-state reaction control of a spacecraft in the presence of environmental disturbance is to ascertain that the control torque always produces a motion which opposes the effect of the disturbing torques. An implication of this statement is that the disturbance must be caused to produce at least one turning point in each limit cycle period. This is optimal in the sense that no control torque is ever required to offset the motion produced by a previous firing. Having established this criterion, the number of thruster ignitions is reduced by causing the vehicle to "coast" after a firing for some maximum time which depends on the environment and on the size of the deadbands.

Regetz and Nelson⁽²⁾ have shown for a single-axis inertial plant subjected to a constant disturbance torque that the control which minimizes the firings is that which causes the spacecraft to just miss contacting the opposite side of the deadband. Smaller than optimal control torque will still yield a minimum-fuel solution if the control opposes the disturbance. There will be, however, an increased number of ignitions. A control torque which exceeds the optimal will cause the vehicle to contact the opposite deadband and result in a firing which produces a motion in the same direction as the disturbance.

* These assumptions are considered in further detail in Section V.

III. AN ILLUSTRATIVE EXAMPLE

Consider the dynamical system represented by the relation:

$$I\ddot{x} = T_D \sin \omega_0 t + T_c(t) \mu(t-t^*) \quad (1)$$

where

- I = moment of inertia about the X axis
- \ddot{x} = angular acceleration about the X axis
- T_D = amplitude of disturbance torque
- $T_c(t)$ = control torque
- ω_0 = radian frequency of disturbance

$$\mu(t-t^*) = \begin{cases} 1 & t^* < t < t_2 \\ 0 & t_2 < t < t^* \end{cases}$$

Dividing through by I and considering T_c to be a constant, equation (1) becomes

$$\ddot{x} = \lambda_D \sin \omega_0 t \pm \lambda_c \mu(t-t^*) \quad (2)$$

Integrating from t_1 , a time before thruster ignition, to $t > t_2$, the instant at which thruster firing is terminated, yields

$$\dot{x}(t) = \left[\left(\dot{x}(t_1) + \frac{\lambda_D}{\omega_0} \cos \omega_0 t_1 \right) \pm \lambda_c t_{on} \right] - \frac{\lambda_D}{\omega_0} \cos \omega_0 t \quad (3)$$

where $t_{on} \triangleq t_2 - t^*$. If the term in parentheses is set equal to $\dot{\epsilon}(t_1)$ and another integration is performed, equation (3) evolves into

$$x(t) = \left\{ \left(x(t_1) + \frac{\lambda_D}{\omega_0^2} \sin \omega_0 t_1 \right) + \dot{\epsilon}(t_1)(t_2 - t_1) \right. \\ \left. + \frac{\lambda_c t_{on}^2}{2} - \frac{\lambda_D}{\omega_0^2} \sin \omega_0 t \right\} \quad (4)$$

Define $n(t_1)$ equal to the term in parentheses in equation (4). Then,

$$x(t) = \left\{ \left[n(t_1) + \dot{\epsilon}(t_1)(t_2 - t_1) + \frac{\lambda_c t_{on}^2}{2} \right] \right. \\ \left. - \frac{\lambda_D}{\omega_0^2} \sin \omega_0 t \right\} \quad (5)$$

If t_{on} , t_2 , and the sign of λ_c can be chosen to null the bracketed terms in equations (3) and (5), then the state equations for a time $t > t_2$,

$$\begin{cases} x(t) = -\frac{\lambda_D}{\omega_0^2} \sin \omega_0 t \\ \dot{x}(t) = -\frac{\lambda_D}{\omega_0} \cos \omega_0 t \end{cases} \quad (6)$$

define the motion of a harmonic oscillator. Notice that all future turning points in the trajectory of this model are produced by the disturbing torques and the amplitude of the oscillation is proportional to λ_D .

In order to formulate a precise conclusion from this example, the following definitions are made:

1) Ideal System

An ideal system is one:

- i) whose inertia is constant and known exactly,
- ii) which is able to measure T_D , ω_0 , t and the state (x and \dot{x}) perfectly, and
- iii) which is able to control the state perfectly.

2) Constant Environment

An environment is defined to be constant if ω_0 and T_D are invariant with time.

Conclusion

If the dynamical system given above is considered to be ideal and in a constant environment, no further control action is required after initialization.

Of course, no system is ideal and the environment which will influence the OA is not constant. There will, therefore, be some thruster activity. However, as shown in Section IV, the environment has periodic properties which can be treated in a manner which is entirely analogous to this example.

IV. APPLICATION TO AAP 1/2 AND AAP 2/3A

Missions AAP 1/2 and AAP 2/3A are scheduled to fly in the POP mode which is defined here by the following coordinate system:

- X - lies along the intersection of the orbital plane and the noon meridian plane, positively directed toward the sun.

Z - perpendicular to the orbital plane (POP). Positive direction makes acute angle with the North Pole of the Earth.

Y - completes the orthogonal right triad.

The Euler angle sequence which defines the spacecraft axes (x, y, and z) relative to X, Y and Z is given by:

- 1) ψ (roll) about the Z axis,
- 2) θ (pitch) about the new Y axis,
- 3) ϕ (yaw) about the new X axis.

This sequence is described more precisely if a transformation symbol is defined. Let T_i^v represent a positive rotation about the i^{th} axis through an angle v . If \underline{x}_I is a vector defined in the inertial system and $\underline{x}_{s/c}$ is the same vector measured relative to the spacecraft coordinate system, then

$$\underline{x}_{s/c} = T_x^\phi T_y^\theta T_z^\psi \underline{x}_I \quad (7)$$

The linearized equations of motion for the OA in circular orbit and acted upon by gravity-gradient and aerodynamic torques* are given by:

$$a) \quad \ddot{\psi} = 2\alpha_z^2 \psi \cos 2\omega_0 t - \alpha_z^2 \sin 2\omega_0 t \quad (8)$$

$$b) \quad \ddot{\theta} = \left\{ \alpha_y^2 \left[\theta(1 + \cos 2\omega_0 t) - \phi \sin 2\omega_0 t \right] + \lambda_y^c \sin(\omega_0 t - \psi) \right. \\ \left. + \lambda_y^p |\sin(\omega_0 t - \psi)| \sin(\omega_0 t - \psi) \right\} \quad (8)$$

* This particular form for the aerodynamic torque results from considering the OA to be a cylinder with rectangular solar panels. However, this model is not essential to the proposed control strategy. All that is necessary is that the aerodynamic torque acting on the spacecraft be expressible in a Fourier series. The diurnal bulge is not included in this model but is discussed in Section V.

$$c) \ddot{\phi} = \left\{ \alpha_x^2 \left[\phi(1 - \cos 2\omega_0 t) - \theta \sin 2\omega_0 t \right] + \lambda_x^c \cos(\omega_0 t - \psi) + \sigma_r \lambda_x^p |\sin(\omega_0 t - \psi)| |\cos(\omega_0 t - \psi)| \right\} \quad (8)$$

where

$$\alpha_x^2 = \frac{3\omega_0^2}{2} \frac{(I_y - I_z)}{I_x}$$

$$\alpha_y^2 = \frac{3\omega_0^2}{2} \frac{(I_x - I_z)}{I_y}$$

$$\alpha_z^2 = \frac{3\omega_0^2}{2} \frac{(I_x - I_y)}{I_z}$$

λ_i^c = maximum value of aero torque acting about the i^{th} axis on the cylindrical portion of the spacecraft divided by appropriate principal moment of inertia

λ_i^p = maximum value of aero torque on the solar panels about the i^{th} axis divided by appropriate principal moment of inertia

σ_r = a coefficient of reflectivity⁽⁶⁾

Although equations (8) are significantly more complicated than the example given in Section III, they are amenable to the same type of solution. That is, assuming an ideal system in a constant environment, proper initialization of the state of the system results in an oscillatory type motion about all three axes. Further, all turning points are caused by the environment and, ideally, no further firing is required.

The technique for determining the "natural" oscillatory type motion of the spacecraft is as follows:

- 1) Solve equation (8a) by the method of successive approximations. Determine the initial values of ψ and $\dot{\psi}$ such that $\psi(t)$ is a libration. This is done in detail in Appendix A.
- 2) Using the derived value of ψ , solve equations (8b) and (8c) by the method of successive approximations. Determine the initial value of the four-dimensional state vector $(\theta, \dot{\theta}, \phi, \dot{\phi})$ such that the motions $\phi(t)$ and $\theta(t)$ are oscillatory. The amplitudes of these oscillations are functions of the appropriate λ 's and α 's.

The results of this analysis using AAP 1/2 moments of inertia⁽³⁾ and assuming an average atmospheric density* of 0.7×10^{-14} slugs/ft³ and a 210 nautical mile circular orbit are:

$$\begin{aligned}\psi(t) &= 9.7 \sin 2\omega_0 t \text{ deg} \\ \theta(t) &= -4.2 \sin \omega_0 t \text{ deg} \\ \phi(t) &= -3.05 \cos \omega_0 t \text{ deg}\end{aligned}\tag{9}$$

To verify the validity of the linear analysis, a simulation was run which used the same environment as above but with the exact, nonlinear equations of motion. The results, given in Figures (1a) and (1b) in Appendix B, are seen to be quite close to the results of the linear analysis, equations (9).

V. PRACTICAL CONSIDERATIONS

In an effort to achieve mathematical simplicity, several assumptions have been made. It is the purpose of this section to review these assumptions and discuss their effects on the design of a practical thruster firing control law.

The assumption of a constant environment is, of course, crude. In particular the aerodynamic disturbance exhibits considerable variation with orbital position, altitude, and solar activity. A linear analysis including the effects of the

* The density assumed is the MSFC +20 estimate at the midpoint of the AAP 1/2 mission.

diurnal bulge revealed that the aerodynamic torque equation included a constant term. This results in an accumulation of angular momentum which must be dumped from time to time. (2) If this dumping is done in the manner of Regetz and Nelson, initial values for the state can still be chosen in a way such that the environment produces two turning points per period of the motion. Figures (2a) and (2b) are the results of the simulation described above with the atmospheric density taken to be

$$\rho = \left[0.7 + 0.45 \cos(\omega_0 t - \gamma) \right] \times 10^{-14} \text{ slugs/ft}^3 \quad (10)$$

where γ locates the peak of the diurnal bulge in the orbital day.

The two essential properties of a control regime then are an ability to determine the aerodynamic torque acting on the spacecraft and a numerical strategy for obtaining the desired initial state. For example the torque may be determined by calculating the angular accelerations from the rate information supplied by the rate sensor package and inserting them into the equations of motion.* The storage of successive values of the aerodynamic torque would enable its periodic properties to be calculated by Fourier techniques. Then a strategy which periodically nulled the average value of the angular momentum can be considered. Note that the continual updating of the properties of the aerodynamic torque and the subsequent reevaluation of the desired initial state can be thought of as an adaptive control policy.

The second assumption made was that the system is ideal. Some of the deviations from the ideal that can be expected in any attitude control system are: uncertainties in the values of the moments of inertia, uncertainties in the location of the principal axes, sensor errors in the measurement of the state vectors, and the imperfection in the ability of the controller to achieve the desired state exactly. Also, as in any system, the effects of these errors are not immediately apparent. A full simulation which utilizes the actual control policy is needed to determine these effects on the performance of the policy. The exact determination of a control law and the development of a simulation are the principal goals in the subsequent investigation.

*The gravity-gradient torque can be calculated from attitude information.

BELLCOMM, INC.

- 10 -

ACKNOWLEDGEMENT

The excellent programming assistance of Mrs. Nancy I. Kirkendall is appreciatively acknowledged.

J. J. Fearnside
J. J. Fearnside

1022-JJF-ep

Attachments
References
Appendices A-B

BELLCOMM, INC.

REFERENCES

1. "Instrument Unit Applications for Saturn I Workshop," MSFC No. III-6-602-91, IBM No. 68-220-0002 (Volume II), July 31, 1968.
2. Regetz, J. D. Jr. and Nelson, T. M., "Feasibility Study of Optimum On-Off Attitude Control System for Spacecraft," NASA TN D-4519, April 1968.
3. "Mass Characteristics for the Cluster Mission," R-P&VE-VAW-67-176, December 26, 1967. (Case 10)
4. Struble, R. A., "Nonlinear Differential Equations," McGraw-Hill Book Company, Inc., 1962, pp. 41-45.
5. Bellman, R., "Adaptive Control Processes: A Guided Tour," Princeton University Press, 1961, pp. 233-234.
6. Schaaf, S. A. and Chambré, P. L., "Flow of Rarefied Gases," Princeton University Press, 1961, pp. 9-11.

BELLCOMM, INC.

APPENDIX A -- THE METHOD OF SUCCESSIVE APPROXIMATIONS

This method is a standard approach in the solution of differential equations when the initial conditions are specified. Struble⁽⁴⁾ provides a rigorous exposition of the method, but it is more simply stated by Bellman.⁽⁵⁾ Following Bellman, then, consider the scalar differential equation

$$\frac{du}{dt} = g(u,t), u(0) = c \quad (A-1)$$

Let $u_0(t)$ be an initial guess and let $u_1(t)$ be determined as the solution of the differential equation

$$\frac{du_1}{dt} = g(u_0,t), u_1(0) = c \quad (A-2)$$

In general, a sequence of functions $\{u_n(t)\}$ can be generated by means of the recurrence relationship,

$$\frac{du_n}{dt} = g(u_{n-1},t), u_n(0) = c \quad (A-3)$$

Equation (A-3) can now be written as an integral equation,

$$u_n(t) = \int_0^t g(u_{n-1},s)ds + c \quad (A-4)$$

and under reasonable assumptions concerning $g(u,t)$, it can be shown that the sequence $\{u_n(t)\}$ converges to the solution of (A-1) in some interval $[0, t_0]$.

These techniques are applied to the roll motion equation (9a) with one change; the control is assumed able to specify a set of initial conditions. Following the example in Section III, the problem is essentially to find the initial state vector which results in an oscillatory roll motion. The initial time, t_1 , is taken to be zero. Rewriting (8a),

$$\ddot{\psi} = 2\alpha_z^2 \psi \cos 2\omega_0 t - \alpha_z^2 \sin 2\omega_0 t \quad (\text{A-5})$$

FIRST APPROXIMATION - $\psi_0 = \psi_1(0) = 0$, $\dot{\psi}_0 = \dot{\psi}_1(0)$ to be determined

$\psi_0 = 0$ implies that (A-5) can be written,

$$\ddot{\psi}_1 = -\alpha_z^2 \sin 2\omega_0 t \quad (\text{A-6})$$

Integrating from 0 to t ,

$$\dot{\psi}_1 = \left(\dot{\psi}_1(0) - \frac{\alpha_z^2}{2\omega_0} \right) + \frac{\alpha_z^2}{2\omega_0} \cos 2\omega_0 t \quad (\text{A-7})$$

Selecting $\dot{\psi}_1(0) = \frac{\alpha_z^2}{2\omega_0}$ and integrating once more yields

$$\psi_1 = \frac{\alpha_z^2}{4\omega_0^2} \sin 2\omega_0 t, \text{ since } \psi_1(0) = 0 \quad (\text{A-8})$$

SECOND APPROXIMATION - $\psi = \psi_1$, $\psi_2(0) = 0$, $\dot{\psi}_2(0) = \dot{\psi}_1(0)$

$$\ddot{\psi}_2 = -\alpha_z^2 \sin 2\omega_0 t + \frac{\alpha_z^4}{4\omega_0^2} \sin 4\omega_0 t \quad (\text{A-9})$$

$$\dot{\psi}_2 = \frac{\alpha_z^2}{2\omega_0} \cos 2\omega_0 t - \frac{\alpha_z^4}{16\omega_0^3} \cos 4\omega_0 t + \frac{\alpha_z^4}{16\omega_0^3} \quad (\text{A-10})$$

$$\psi_2 = \frac{\alpha_z^2}{4\omega_0^2} \sin 2\omega_0 t - \frac{\alpha_z^4}{64\omega_0^4} \sin 4\omega_0 t + \frac{\alpha_z^4}{16\omega_0^3} t \quad (\text{A-11})$$

There are several observations which may be made at this point:

- 1) A better selection for $\dot{\psi}_2(0)$ is $\dot{\psi}_1(0) - \frac{\alpha_z^4}{16\omega_0^3}$
- 2) If $\alpha_z^2/\omega_0^2 < 1$ (as it is for the parameters of the OA) then $|\psi_2 - \psi_1| < |\psi_1 - \psi_0|$ and the series is converging to $\psi(t)$.

THIRD APPROXIMATION -- $\psi = \psi_2$, $\psi_3(0) = 0$

$$\ddot{\psi}_3 = \left\{ \begin{array}{l} -\alpha_z^2 \left(1 + \frac{\alpha_z^4}{64\omega_0^4} \right) \sin 2\omega_0 t + \frac{\alpha_z^4}{4\omega_0^2} \sin 4\omega_0 t \\ - \frac{\alpha_z^6}{64\omega_0^4} \sin 6\omega_0 t \end{array} \right\} \quad (\text{A-12})$$

If $\dot{\psi}_3(0) = \frac{\alpha_z^2}{2\omega_0} - \frac{\alpha_z^4}{16\omega_0^3} + \frac{\alpha_z^6}{96\omega_0^5}$, then

$$\dot{\psi}_3 = \left\{ \begin{array}{l} \frac{\alpha_z^2}{2\omega_0} \left(1 + \frac{\alpha_z^4}{64\omega_0^4} \right) \cos 2\omega_0 t - \frac{\alpha_z^4}{16\omega_0^3} \cos 4\omega_0 t \\ + \frac{\alpha_z^6}{384\omega_0^5} \cos 6\omega_0 t \end{array} \right\} \quad (\text{A-13})$$

$$\psi_3 = \left\{ \frac{\alpha_z^2}{4\omega_0^2} \left(1 + \frac{\alpha_z^4}{64\omega_0^4} \right) \sin 2\omega_0 t - \frac{\alpha_z^4}{64\omega_0^3} \sin 4\omega_0 t + \frac{\alpha_z^6}{2304\omega_0^6} \sin 6\omega_0 t \right\} \quad (\text{A-14})$$

To get a physical "feel" for the rapidity of convergence, the parameters of the OA are inserted into (A-14). The result is:

$$\psi_3 = \left\{ 0.1696 \sin 2\omega_0 t - 0.007 \sin 4\omega_0 t + 0.00013 \sin 6\omega_0 t \right\} \quad (\text{A-15})$$

Considering just the first term, the amplitude of ψ_3 is .1696 radians which corresponds to 9.7° . Similarly $\dot{\psi}_3 \approx 20 \times 10^{-3}$ degrees/second maximum.

The application of this method to the simultaneous solution of the x and y axis motion yields the results stated in the introduction.

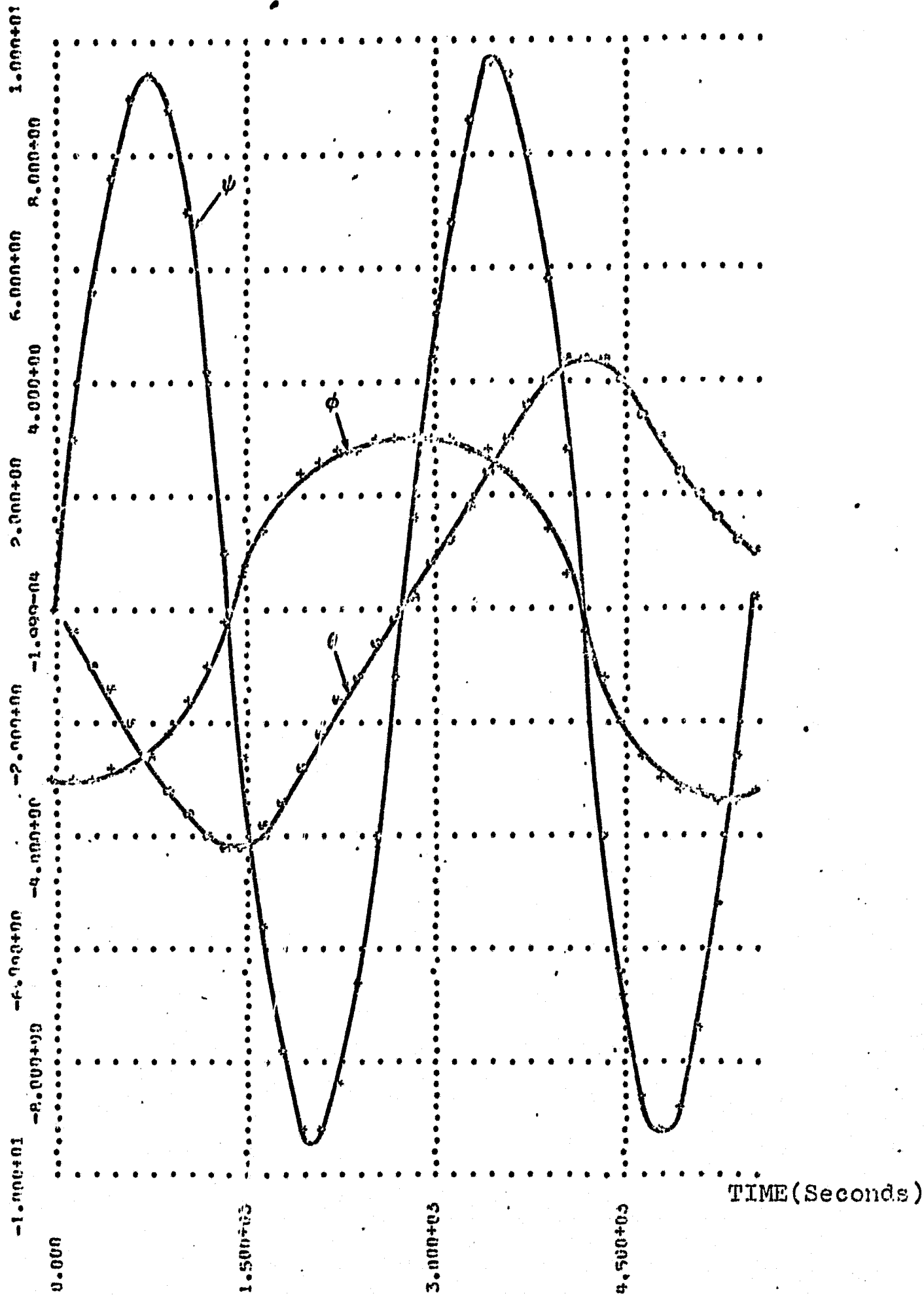
APPENDIX B

TIME	PHI	THE	PSI	OM1	OM2	OM3
.00000	-.291000+01	.000000	.000000	.000000	-.407000-02	.195000-01
.150000+03	-.291233+01	-.464140-00	.290816+01	.138085-03	-.408360-02	.186166-01
.300000+03	-.290763+01	-.944757-00	.552283+01	.370739-03	-.410621-02	.159846-01
.450000+03	-.287131+01	-.145430+01	.767639+01	.719018-03	-.409977-02	.116763-01
.600000+03	-.275970+01	-.199735+01	.903838+01	.119373-03	-.401006-02	.587075-02
.750000+03	-.256259+01	-.256476+01	.943704+01	.178473-02	-.376808-02	-.106195-02
.900000+03	-.221032+01	-.312698+01	.374491+01	.244473-02	-.330821-02	-.847051-02
.105000+04	-.168739+01	-.363028+01	.695560+01	.309356-02	-.255227-02	-.153825-01
.120000+04	-.100036+01	-.400294+01	.422959+01	.359865-02	-.152487-02	-.206124-01
.135000+04	-.200343-00	-.417613+01	.906706-00	.384079-02	-.300495-03	-.230733-01
.150000+04	.623662-00	-.411294+01	-.253932+01	.375312-02	.966266-03	-.221943-01
.165000+04	.137391+01	-.382691+01	-.560516+01	.336063-02	.210395-02	-.181833-01
.180000+04	.197883+01	-.337495+01	-.787664+01	.276576-02	.299142-02	-.119299-01
.195000+04	.241126+01	-.283071+01	-.910552+01	.209828-02	.359093-02	-.662075-02
.210000+04	.268374+01	-.225876+01	-.922217+01	.146648-02	.393547-02	.264262-02
.225000+04	.283142+01	-.169794+01	-.330190+01	.935516-03	.409380-02	.905234-02
.240000+04	.289574+01	-.118820+01	-.651616+01	.530179-03	.413976-02	.141132-01
.255000+04	.291421+01	-.669673-00	-.409038+01	.247821-03	.413575-02	.175662-01
.270000+04	.291599+01	-.192382-00	-.127378+01	.708374-04	.412799-02	.192963-01
.285000+04	.292025+01	.278460-00	.166611+01	.440692-04	.410672-02	.192634-01
.300000+04	.292631+01	.761212-00	.447127+01	-.227319-03	.419164-02	.174583-01
.315000+04	.291392+01	.127126+01	.687837+01	-.520404-03	.423253-02	.159329-01
.330000+04	.285259+01	.181843+01	.863675+01	-.942335-03	.422277-02	.883587-02
.345000+04	.270296+01	.240184+01	.952243+01	-.149740-02	.409359-02	.238593-02
.360000+04	.242127+01	.300392+01	.936660+01	-.216210-02	.378382-02	-.489772-02
.375000+04	.196989+01	.357948+01	.809807+01	-.287145-02	.320649-02	-.121895-01
.390000+04	.133442+01	.406475+01	.579195+01	-.351540-02	.233056-02	-.183823-01
.405000+04	.541765-00	.438204+01	.270279+01	-.396018-02	.119219-02	-.222916-01
.420000+04	-.334578-00	.447195+01	-.750051-00	-.409740-02	-.862106-04	-.230482-01
.435000+04	-.119316+01	.432040+01	-.406157+01	-.389586-02	-.132833-02	-.204731-01
.450000+04	-.194047+01	.396623+01	-.676045+01	-.341626-02	-.237100-02	-.151617-01
.465000+04	-.252090+01	.348247+01	-.851242+01	-.277659-02	-.311988-02	-.821144-02
.480000+04	-.292376+01	.294676+01	-.916379+01	-.209828-02	-.355989-02	-.804031-03
.495000+04	-.317066+01	.241998+01	-.872634+01	-.146947-02	-.372884-02	.609964-02
.510000+04	-.329742+01	.193999+01	-.733181+01	-.936646-03	-.368259-02	.118597-01
.525000+04	-.334054+01	.152546+01	-.518478+01	-.514515-03	-.347087-02	.161153-01
.540000+04	-.333056+01	.118325+01	-.252741+01	-.201013-03	-.312689-02	.166925-01
.554013+04	-.329392+01	.930311-00	.187689-00	-.138580-05	-.269999-02	.195211-01

EULER ANGLES AND BODY RATES VS TIME FOR 1 ORBIT OF THE AAP CLUSTER IN POP MODE

FIGURE 1(a)

EULER ANGLES FOR AAP CLUSTER IN POP MODE (Degrees)

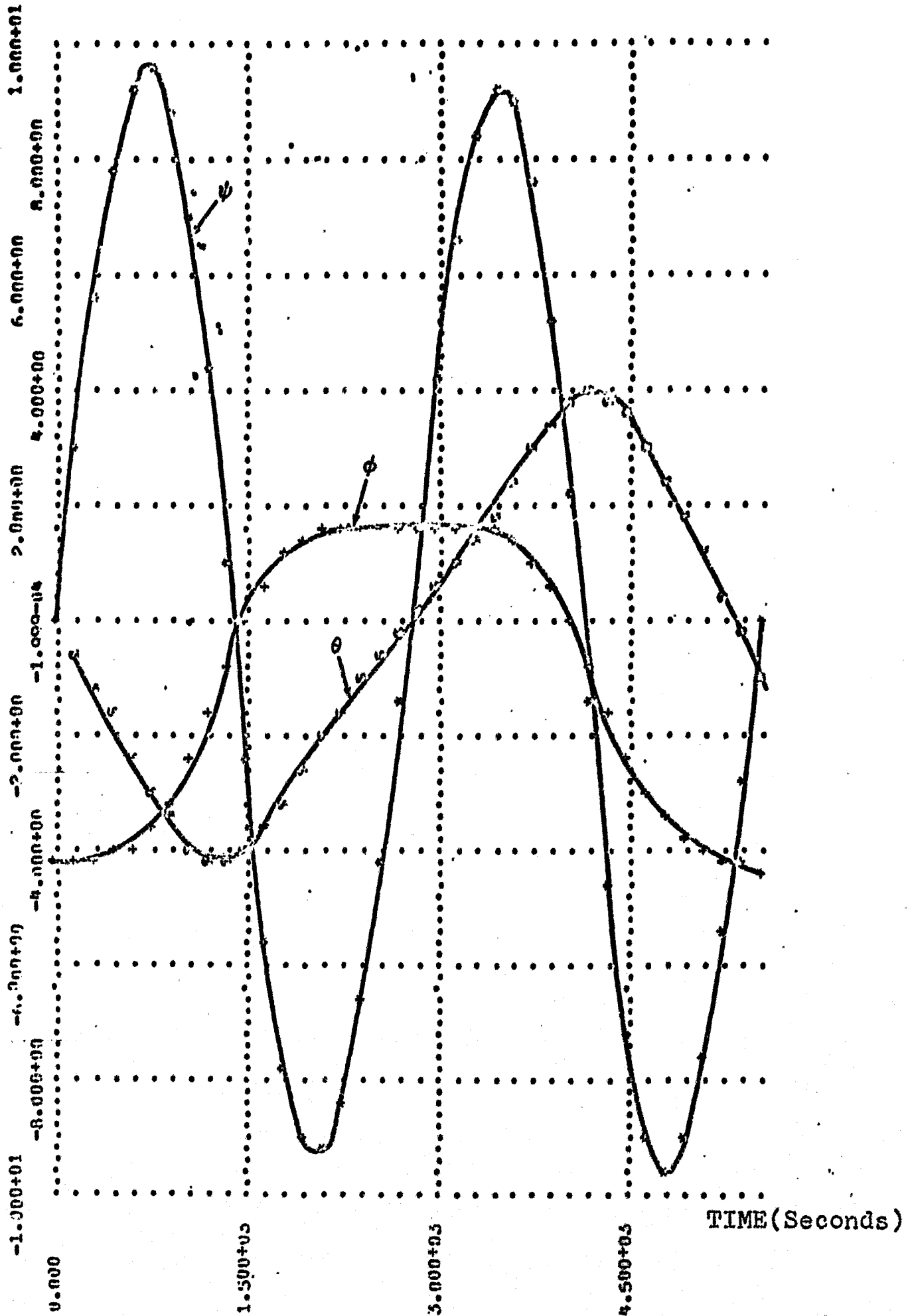


TIME	PHI	THF	PST	OM1	OM2	OM3
.000000	-.422500+01	.000000	.000000	.000000	-.509000-02	.195000-01
.150000+03	-.421919+01	-.540576-00	.292927+01	.282449-03	-.507477-02	.186179-01
.300000+03	-.418611+01	-.111139+01	.559508+01	.689605-03	-.500531-02	.159893-01
.450000+03	-.409602+01	-.160671+01	.773941+01	.122439-02	-.482666-02	.116057-01
.600000+03	-.391247+01	-.230209+01	.912069+01	.167055-02	-.448379-02	.500440-02
.750000+03	-.359690+01	-.290845+01	.953551+01	.258133-02	-.390968-02	-.104652-02
.900000+03	-.311618+01	-.347464+01	.885447+01	.327005-02	-.305473-02	-.085026-02
.105000+04	-.246789+01	-.393752+01	.707026+01	.381293-02	-.191662-02	-.153883-01
.120000+04	-.167670+01	-.422401+01	.454314+01	.407703-02	-.572103-03	-.203274-01
.135000+04	-.820098-00	-.427688+01	.101448+01	.397436-02	.617454-03	-.231899-01
.150000+04	-.149768-02	-.408300+01	-.244053+01	.351310-02	.205120-02	-.222525-01
.165000+04	.684005-00	-.365346+01	-.551839+01	.280468-02	.296874-02	-.182593-01
.180000+04	.118278+01	-.315565+01	-.780562+01	.201231-02	.351027-02	-.129160-01
.195000+04	.149197+01	-.258079+01	-.905461+01	.128395-02	.371764-02	-.471303-02
.210000+04	.164555+01	-.201910+01	-.919543+01	.705751-03	.369040-02	.254655-02
.225000+04	.169250+01	-.150203+01	-.830268+01	.304808-03	.353697-02	.395132-02
.240000+04	.168022+01	-.103732+01	-.654712+01	.663333-04	.330628-02	.140031-01
.255000+04	.164639+01	-.617729-00	-.415418+01	-.445167-04	.317973-02	.174410-01
.270000+04	.161632+01	-.228447-00	-.137567+01	.680986-04	.307496-02	.191303-01
.285000+04	.160534+01	.148614-00	.152580+01	-.515831-04	.305143-02	.193032-01
.300000+04	.161344+01	.532411-00	.428499+01	-.734309-04	.310077-02	.172323-01
.315000+04	.162572+01	.940654-00	.663969+01	-.177632-03	.392733-02	.130092-01
.330000+04	.161784+01	.130752+01	.033929+01	-.402820-03	.337022-02	.053007-02
.345000+04	.155375+01	.187942+01	.916140+01	-.781659-03	.307303-02	.200923-02
.360000+04	.136855+01	.240799+01	.894085+01	-.132692-02	.345364-02	-.524421-02
.375000+04	.107663+01	.294193+01	.761230+01	-.201141-02	.322751-02	-.125136-01
.390000+04	.587897-00	.342288+01	.525801+01	-.270360-02	.267089-02	-.106393-01
.405000+04	-.724689-01	.377357+01	.213299+01	-.340239-02	.178083-02	-.220214-01
.420000+04	-.851193-00	.392219+01	-.132170+01	-.321912-02	.551051-03	-.130352-01
.435000+04	-.165859+01	.303239+01	-.461919+01	-.389900-02	-.301163-03	-.203254-01
.450000+04	-.240033+01	.351822+01	-.726568+01	-.364590-02	-.211940-02	-.199163-01
.465000+04	-.301085+01	.303276+01	-.899241+01	-.314972-02	-.324851-02	-.792033-02
.480000+04	-.346744+01	.244104+01	-.959155+01	-.255512-02	-.414526-02	-.514331-03
.495000+04	-.378304+01	.179640+01	-.910004+01	-.192091-02	-.482164-02	.635243-02
.510000+04	-.399420+01	.112987+01	-.765307+01	-.138446-02	-.333022-02	.120030-01
.525000+04	-.413916+01	.450451-00	-.545678+01	-.964333-03	-.577021-02	.162302-01
.540000+04	-.425553+01	-.250127-00	-.275323+01	-.667028-03	-.618082-02	.187393-01
.554013+04	-.436398+01	-.941755-00	.376462-02	-.485365-03	-.362111-02	.190063-01

EULER ANGLES AND BODY RATES VS TIME FOR 1 ORBIT OF THE AAP CLUSTER IN POP MODE

FIGURE 2 (a)

EULER ANGLES FOR AAP CLUSTER IN POP MODE (Degrees)



Official File Copy
FIGURE 2 (b) (1) (2) (3) (4) (5) (6) (7) (8) (9) (10) (11) (12) (13) (14) (15) (16) (17) (18) (19) (20) (21) (22) (23) (24) (25) (26) (27) (28) (29) (30) (31) (32) (33) (34) (35) (36) (37) (38) (39) (40) (41) (42) (43) (44) (45) (46) (47) (48) (49) (50) (51) (52) (53) (54) (55) (56) (57) (58) (59) (60) (61) (62) (63) (64) (65) (66) (67) (68) (69) (70) (71) (72) (73) (74) (75) (76) (77) (78) (79) (80) (81) (82) (83) (84) (85) (86) (87) (88) (89) (90) (91) (92) (93) (94) (95) (96) (97) (98) (99) (100)